Sedimentology (2006) **53,** 35–53 doi: 10.1111/j.1365-3091.2005.00752.x

Facies distribution of the Lower Cambrian cryptic microbial and epibenthic archaeocyathan-microbial communities, western Anti-Atlas, Morocco

J. JAVIER ÁLVARO*†, SÉBASTIEN CLAUSEN†, ABDERRAZZAK EL ALBANI‡ and EL HASSANE CHELLAI§
**Departamento Ciencias de la Tierra, Universidad de Zaragoza, Zaragoza, Spain (E-mail: jose-javier.alvaro@univ-lille1.fr)*
†LP3, UMR 8014 CNRS, UFR Sciences de la Terre, Université des Sciences et Technologies de Lille, 59655-Villeneuve d'Ascq, France
‡Laboratoire HIDRASA, UMR 6532 CNRS, UFR SFA, Université de Poitiers, 40 av. du Recteur Pineau, 86022-Poitiers, France
§Département de Géologie, Faculté des Sciences-Semlalia, Université de Cadi Ayyad, Marrakech, Morocco

ABSTRACT

Marine microbial communities recorded in the Moroccan Anti-Atlas were unaffected across the Neoproterozoic–Cambrian transition. A stromatolite-dominated consortium was replaced at the beginning of the Atdabanian (*ca* 20 Myr after the Neoproterozoic–Cambrian boundary) by shelly metazoan and thromboid consortia, which contain the oldest biostratigraphically significant fossils of the Moroccan Cambrian. The associated collapse of microbial mat (stromatolitic) growth appears to coincide with a change from pre-Atdabanian shallow-water restricted conditions into Atdabanian deeper, open-sea conditions. It is postulated that this environmental change led to an episode of improved water circulation over carbonate platform interiors, promoting shelly metazoan immigration into the region. The Tiout/Amouslek lithostratigraphic contact in the early Atdabanian marks the end of an episodically unstable seafloor as suggested by the abundance of slumping and sliding structures, and synsedimentary microfaults and cracks recorded in the underlying Tiout Member. Concurrent with the transition is the occurrence of a network of cryptic fissures and cavities that provided habitats for a coelobiontic chemosynthetic–heterotrophic microbial community composed of stromatolitic crusts, *Renalcis–Epiphyton–Girvanella* intergrowths, and *Kundatia* thalli. In the overlying Amouslek Formation, archaeocyathan–thromboid reefs were constrained by substrate stability, water depth and subsidence rate. Four reef geometries are distinguished: (i) patch reefs surrounded by shales, (ii) bioherms in which flank beds intercalate laterally with carbonate and shale inter-reef sediments, (iii) biostromes or low-relief structures formed as a result of lateral accretion of patch reefs, and (iv) kalyptrate complexes that nucleated because of a marked tendency for aggregation, and in which patch reefs and bioherms occur stacked together bounded by clay–marl–silt seams.

Keywords Anti-Atlas, benthic replacement, cryptic cavities, Lower Cambrian, microbialites, reefs.

INTRODUCTION

The pattern of metazoan diversification that took place in the late Neoproterozoic (Ediacaran) and earliest Cambrian was recorded differently in various marine platforms depending upon their geodynamic, environmental and taphonomic conditions (see an updated revision in Zhuravlev & Riding, 2001). However, some geographical barriers on some platforms allowed the microbial (stromatolite–thrombolite) consortium to survive in isolation until middle Early Cambrian times.

One such sample exists in the Moroccan Anti-Atlas, where the marine microbial communities of the Souss Basin (Geyer, 1989) were unaffected across the Neoproterozoic–Cambrian transition. This microbial consortium was maintained through this transition as preserved in the Adoudou, Lie-de-vin and lower member of the Igoudine formations (Schmitt, 1979). In other basins, new groups of algae, heterotrophic protistans and metazoans evolved, and microbial communities declined dramatically in diversity and abundance because of their retreat from many of the subtidal environments that had been most favourable for them. A relic microbial community, however, appears to have been 'protected' in the western Souss platform until the Early Atdabanian, *ca* 20 Myr after the Neoproterozoic–Cambrian boundary. The stromatolite-dominated facies assemblage on the western Souss platform was succeeded in the Early Atdabanian by an abrupt intrusion of shelly facies (Sdzuy, 1978; Monninger, 1979). As a result, the location of the Neoproterozoic–Cambrian boundary (defined by the first appearance of the ichnospecies *Treptichnus pedum*; Narbonne *et al.*, 1987) remains problematical in Morocco because it lies at the base or within a thick carbonate-dominated succession (Adoudou, Lie-de-vin and lower member of the Igoudine formations) that is extremely poor in shelly metazoans and ichnofossils. The boundary is tentatively correlated with radiometric ages and carbon-isotope signatures (Kirshvink *et al.*, 1991; Magaritz *et al.*, 1991; Fig. 1).

The aim of this paper is to better understand the depositional processes that controlled the Early Atdabanian change from restricted to somewhat normal marine conditions and the associated abrupt immigration of shelly metazoans into the western Anti-Atlas. Both events allowed microbial nucleation in cryptic cavities and fissures crosscutting episodically unstable rigid substrates, and development of epibenthic microbial and archaeocyathan–microbial reefs. The latter contain the oldest biostratigraphically significant fossils of the Lower Cambrian sedimentary rocks in Morocco.

GEOLOGICAL SETTING AND STRATIGRAPHY

The Neoproterozoic(?)–Cambrian successions of the Moroccan Atlas are located in the Anti-Atlas and central High-Atlas (Fig. 2), although some disconnected outcrops occur in the Jbilet and Rehamna regions, and the Meseta plateau. The oldest Cambrian shelly metazoans of the Souss Basin occur in limestones and dolostones of the

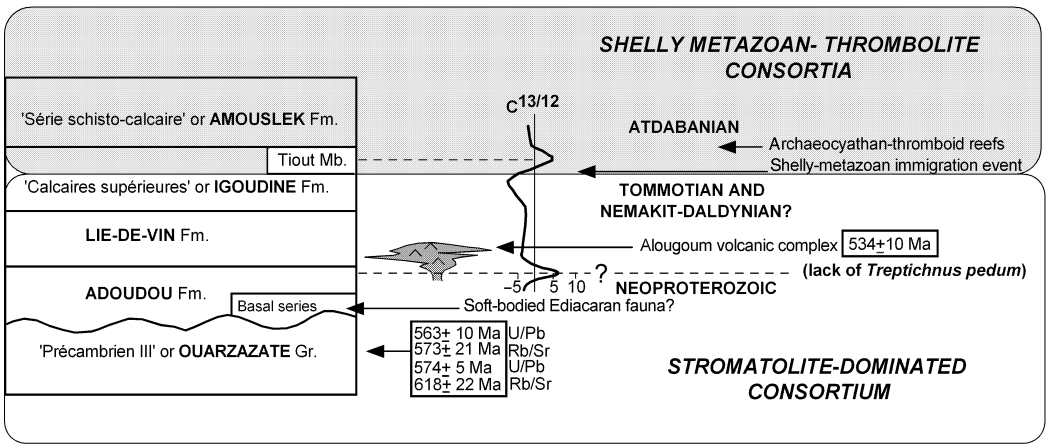

Fig. 1. Stratigraphic framework of the Neoproterozoic–Cambrian transition in the Moroccan Atlas with the chronologic succession of event stratigraphy (summarized after Houzay, 1979; Leblanc & Lancelot, 1980; Clauer *et al.*, 1982; Destombes *et al.*, 1985; Tucker, 1986; Latham & Riding, 1990; Kirshvink *et al.*, 1991; Magaritz *et al.*, 1991; Debrenne & Debrenne, 1995; Geyer *et al.*, 1995; and references therein).

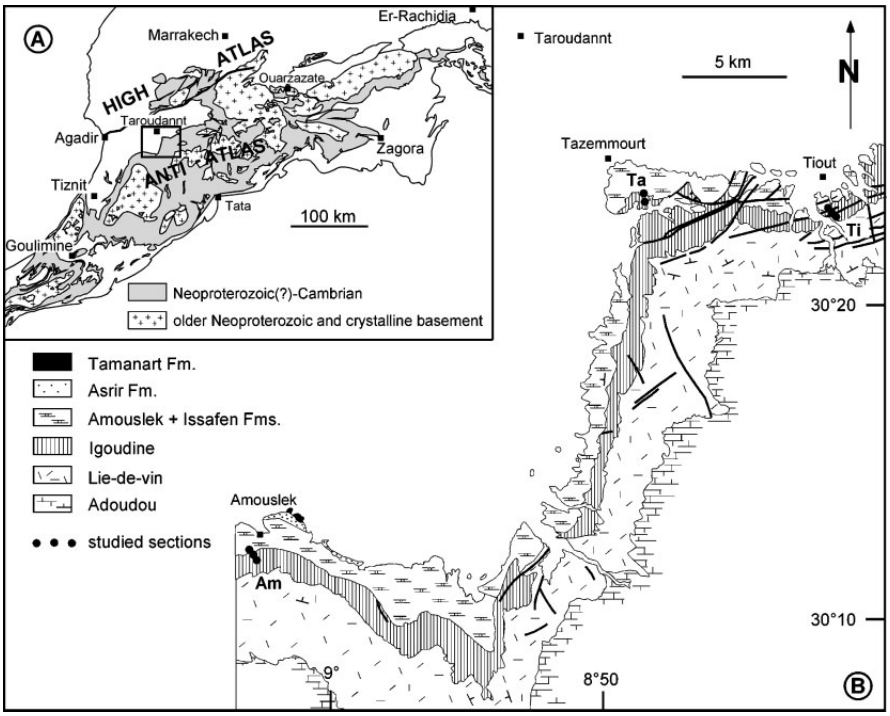

Fig. 2. Geological sketch of (A) the Neoproterozoic(?)–Cambrian outcrops of the High Atlas and Anti-Atlas (modified from Geyer *et al.*, 1995), and (B) setting of the studied sections: Ti, Tiout; Ta, Tazemmourt; and Am, Amouslek (modified from Boudda *et al.*, 1979).

upper member of the Igoudine Formation in the Tiout area and at the bottom of the overlying Amouslek Formation in other outcrops (Geyer *et al.*, 1995; Fig. 3). Both units formed an Early Cambrian carbonate platform that bordered part of the western Gondwana margin (Álvaro *et al.*, 2003).

The *Calcaires supérieures* (Choubert, 1952) or Igoudine Formation (Geyer, 1989), up to 400 m thick, are composed of massive limestones, largely dolomitized at the lower part, locally interbedded with shales and sandstones. An important lithofacies change identified in its stratotype (Tiout section) allows subdivision into two members: (i) an unnamed lower member (*ca* 185 m thick), composed of black, commonly laminated, lime mudstones and dolostones, and (ii) an upper member named the Tiout Member (110 m thick in its stratotype) subdivided by Monninger (1979) and Schmitt (1979) into a 'black oolitic limestone facies' overlain by an 'archaeocyathid–bioherm facies'. As Hupé (1953) identified the top of the *Calcaires supérieures* at the occurrence of shales and archaeocyathan bioherms, it is proposed here to amend the Tiout–Amouslek lithostratigraphic contact by

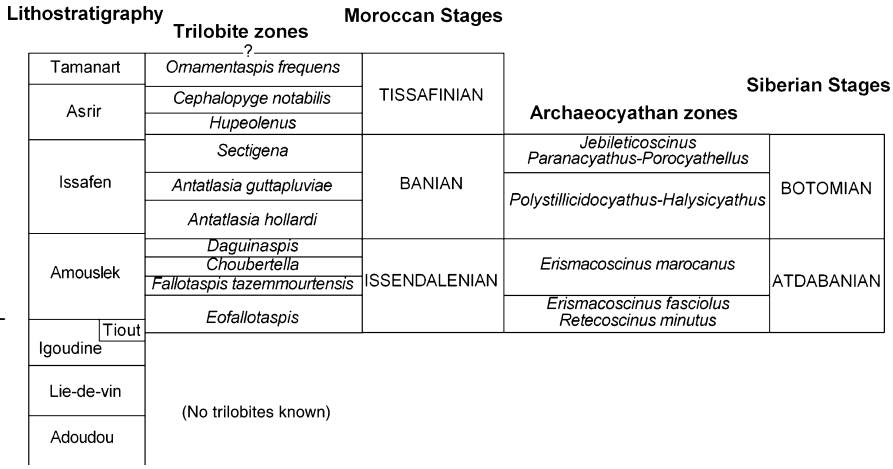

Fig. 3. Neoproterozoic(?)–Lower Cambrian lithostratigraphic and biostratigraphic units of the Amouslek–Tiout area (modified from Geyer *et al.*, 1995), and correlation with the Siberian scale based on archaeocyathans (Debrenne & Debrenne, 1995).

introducing the 'archaeocyathid–bioherm facies' within the Amouslek Formation. This takes into account the sharp contact between the lower black, bedded limestones of the 'oolitic limestone facies' and the nodular aspect of the overlying brownish patch reefs embedded in green shales shown by both the 'archaeocyathid–bioherm' facies and the overlying Amouslek Formation. This boundary is easily mappable and currently used in the geological maps of the Anti-Atlas (see Fig. 3 for lithostratigraphic and biostratigraphic relationships). An Atdabanian age (according to the Siberian chart; Spizharski *et al.*, 1986) of the Tiout Member is based on the occurrence of the oldest Moroccan trilobites (*Eofallotaspis* trilobite zone; Sdzuy, 1978; Geyer, 1990) and archaeocyaths (*Erismacocisnus fasciolus–Retecoscinus minutus* archaeocyathan zone; Debrenne & Debrenne, 1995), and on the carbon-isotope stratigraphy (Latham & Riding, 1990).

The overlying *Série schisto-calcaire* (Choubert, 1952) or Amouslek Formation (Geyer, 1989) is a 40–220 m thick succession of variegated shales with interbedded limestones rich in archaeocyathan–microbial reefs. The formation locally contains abundant trilobites (Hupé, 1953) and archaeocyaths (Debrenne & Debrenne, 1995) that allow subdivision into several Lower Cambrian, archaeocyathan and trilobite zones (Fig. 3).

Three key sections containing the Tiout/Amouslek lithostratigraphic transition, which are the focus of this paper (Fig. 2B), are considered by the *International Subcommission on Cambrian Stratigraphy* as the reference sections of the lowermost part of the Issendalenian Stage (Geyer *et al.*, 1995). The Tiout section [global positioning system (GPS) coordinates 30°23′N/08°41′W of the Taroudannt map sheet] is one of the best-studied Cambrian outcrops in the Anti-Atlas including depositional environments (Monninger, 1979), microbial structures (Schmitt, 1979), trilobites (Sdzuy, 1978), archaeocyaths (last revision in Debrenne & Debrenne, 1995), carbon-isotope curves (Tucker, 1986; Magaritz *et al.*, 1991), magnetostratigraphy (Kirshvink *et al.*, 1991) and trace fossils (Latham & Riding, 1990). The Tazemmourt section (GPS coordinates 30°23′N/08°48′W of the Taroudannt map sheet) is another key section. Abadie (log published in Hupé, 1953) was the first to report its stratigraphy in detail, Hupé (1953) described its trilobites and Debrenne (last revision in Debrenne & Debrenne, 1995) its archaeocyaths. Choubert (1953) was the first to point out the tectonically disturbed aspect of some of the outcrops at the Tazemmourt section. Finally, the Amouslek section (GPS coordinates 30°11′N/09°02′W of the Aït Baha map sheet) is one of the most complete stratigraphic references of the Moroccan Lower Cambrian. Its lithostratigraphy and biostratigraphy have been successively improved from Hupé's (1953) pioneer work by Destombes *et al.* (1985), Geyer (1989, 1990) and Geyer *et al.* (1995), among others.

FACIES ASSOCIATIONS OF THE TIOUT MEMBER

The facies associations described below crop out up to 100 m below the amended Tiout/Amouslek lithostratigraphic contact. Figure 4 shows the stratigraphic logs, whereas the small-scale sequence types or parasequences (*sensu* Van Wagoner *et al.*, 1988) are shown in Fig. 5.

Stromatolitic reefs

This facies association was previously reported as 'type 4 of reefal growth framework' by Monninger (1979) and 'cumulate stromatolites' by Geyer *et al.* (1995), and is only recognizable directly underlying the 'black oolitic limestone facies' at the Tiout section. Monninger (1979) described the facies association as 'very irregular to bulbous, centimetre-sized heads, irregularly laminated, *Nimbophyton*-type (Schmitt, 1979) stromatolites, with finely crystalline, impure dolostone (locally limestone) as host rocks'. Some parasequences (0·3–1 m thick) have, at their base, slumped, contorted, brecciated and faulted stromatolitic and peloidal-rich laminae (Fig. 6A and B). Crinkled stromatolites comprise the bulk of the parasequences, which accrete vertically to produce dome-shaped stromatolites, up to 1 m in diameter. Interdomal areas are either filled with fine-grained peloidal packstones to wackestones, or host smaller domal and crinkled stromatolites that are gradually enveloped by the larger accreting domes. Finally, synoptic relief diminishes upwards, where domes are covered by dolomudstones displaying desiccation cracks, tepee structures and scalloped surfaces (see detailed descriptions in Schmitt, 1979).

The superposition of parasequences is interpreted as repeated asymmetric shallowing-upward events. Each parasequence commences with an initial phase of rapid deepening and is followed by gradual stromatolite accretion, from crinkled to dome-shaped morphologies. The uppermost part of some parasequences provides

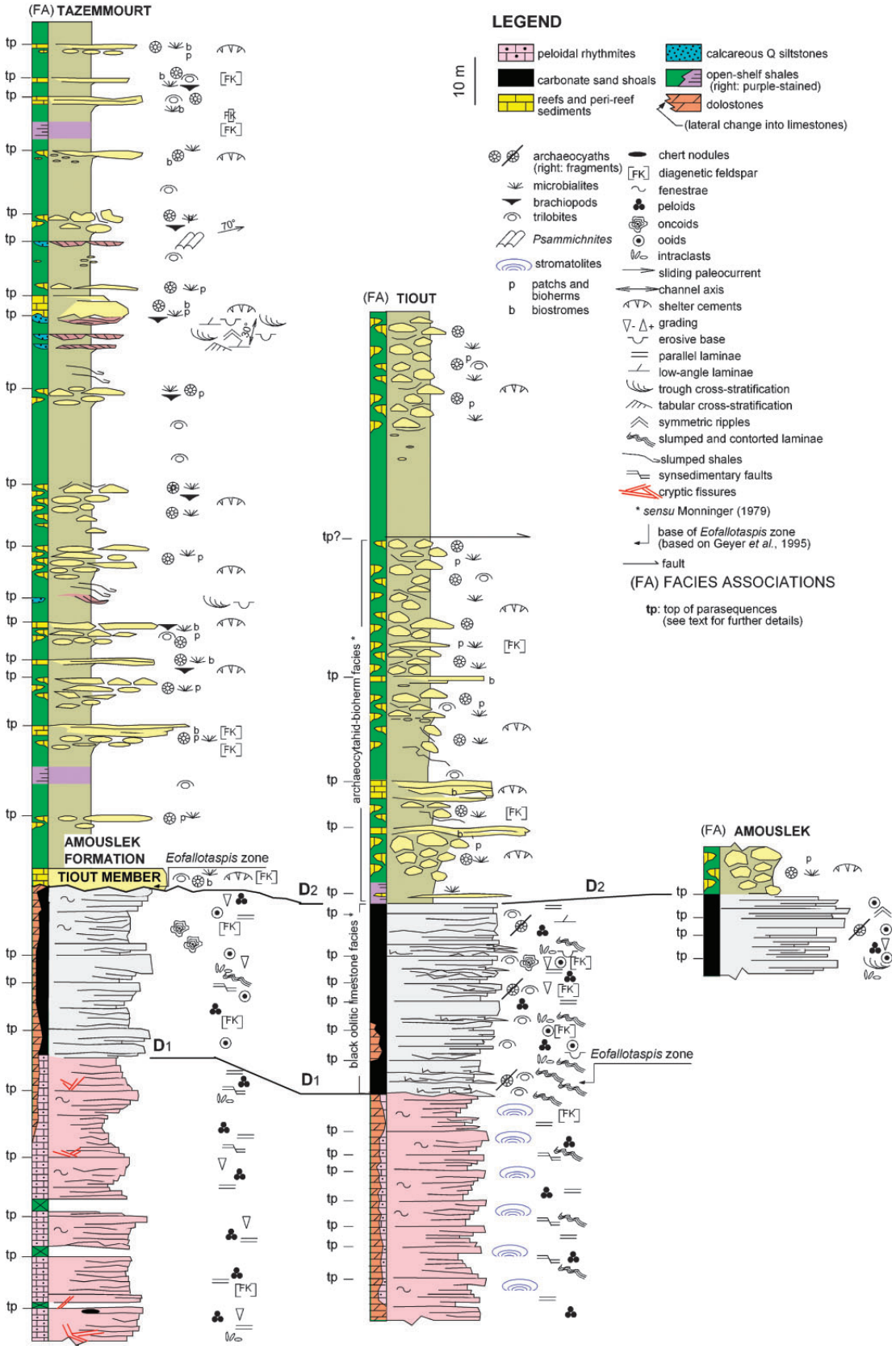

Fig. 4. Stratigraphic sections of Tiout, Tazemmourt and Amouslek (see text for more details). The facies of the cryptic fissures found in the Tiout Member at Tazemmourt are not described in the figure.

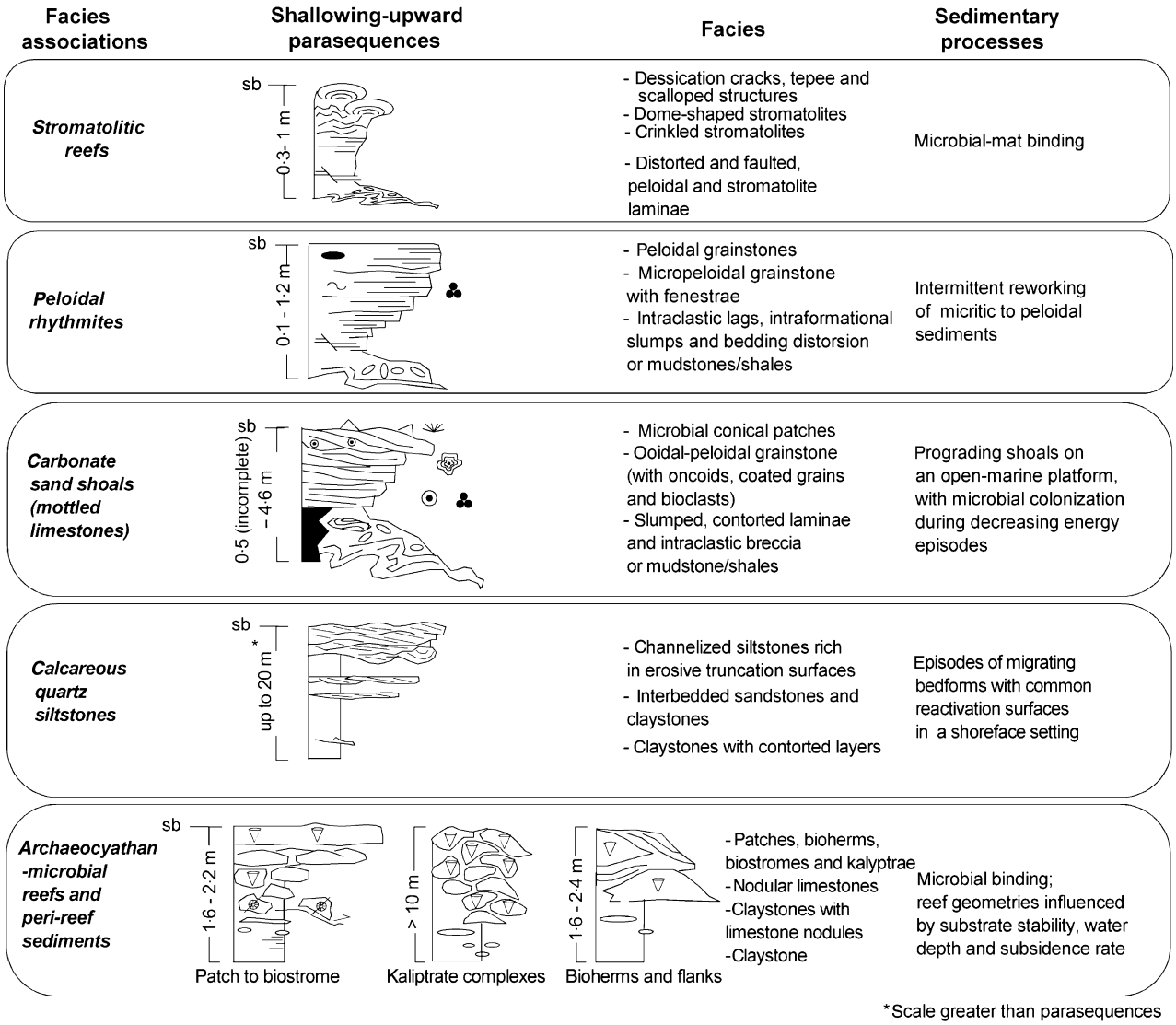

Fig. 5. Basic small-scale sequences or parasequences described in the text, and summary of major depositional systems.

evidence for subaerial exposure although the stromatolite reefs appear to have commonly developed in shallow-water, peritidal environments. The tops of the parasequences are marked by erosive surfaces associated with subsequent transgression (Fig. 5) that was related to episodes of seafloor instability that affected both consolidated and unconsolidated biomats.

Peloidal rhythmites

The rhythmites define well-bedded asymmetric parasequences (0·1–1·2 m thick) recognized as tabular units traceable over several tens of metres in outcrop. From bottom to top, the parasequences contain an intraclastic lag, micropeloidal grainstone alternations (Fig. 6C), and peloidal grainstones. The intraclastic lag (up to 0·1 m thick), which occurs overlying scoured bases with flame structures, are clast-supported and typically disorganized. Clasts are randomly oriented, angular in shape, and commonly comprise grainstones of peloids and peloidal aggregates. They are laterally associated with centimetre-thick, intraformational slumps, synsedimentary bedding distortion, and microfaulting rich in truncation and onlapping surfaces. The overlying millimetre-thick alternations (up to 1·1 m thick) show undulatory- and planar-laminar bedding, rare low-angle cross-laminae, irregular laminoid (fenestral) fabrics, and numerous low-angle erosive surfaces (up to 4 cm deep) directly onlapped

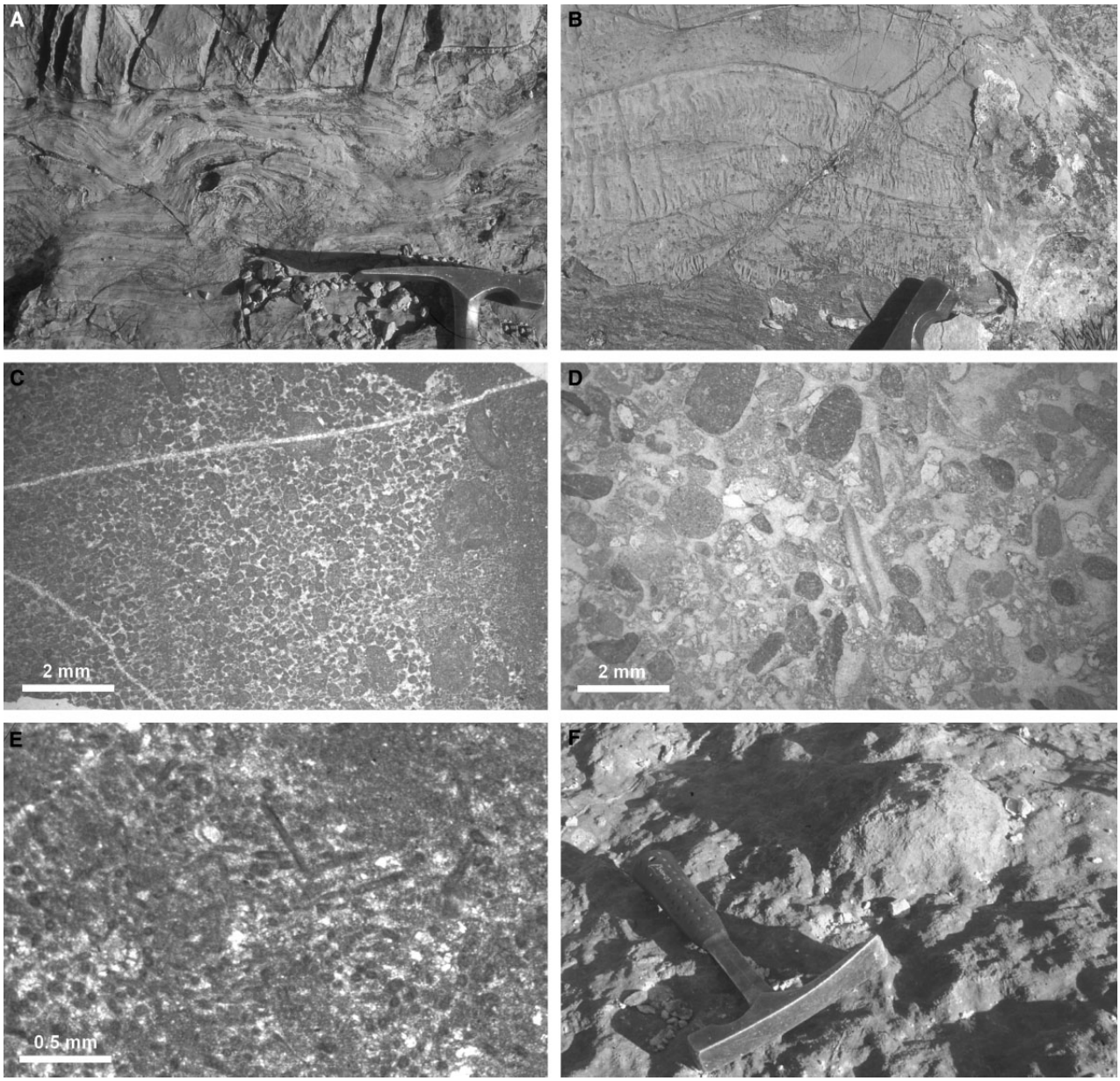

Fig. 6. Field and photomicrographs of representative facies. (A) Slumped stromatolite and peloidal-rich layers at the bottom of the stromatolitic parasequences at Tiout; (B) synsedimentary fracture affecting consolidated stromatolites at the bottom of the stromatolitic parasequences at Tiout; (C) micropeloidal to peloidal grainstones and packstones (top on the left) at Tazemmourt; (D) aggregate-rich grainstone of the mottled limestones at Amouslek; (E) microbial (*Proaulopora*) grainstones in the mottled limestones at Amouslek; (F) centimetre-thick, microbial patch overlying the ooidal shoals.

by rhythmites. The dark laminae (< 2 mm thick) are essentially micropeloidal packstones to wackestones, whereas the light laminae (up to 8 mm thick) consist of micropeloidal grainstones. They are composed of 70–80% micropeloids (200–400 μm in diameter), 5–10% subangular intraclasts (up to 600 μm in diameter), and 5–10% quartz silt, along with several generations of fine, equant to bladed calcite cements occluding interparticle pores. These alternations pass gradually upwards into alternations (1–10 cm thick) of medium-sorted, peloidal grainstones and packstones, with angular to subangular peloids that are up to 3 mm in diameter.

The sorting, roundness, grading, alternating laminae and basal erosive surfaces of the parasequences suggest intermittent reworking of micritic to peloidal sediments in a medium- to high-energy subtidal environment. The intraclastic lags appear to have formed by disruption and

erosion of the coherent thin rhythmic layers, which were accumulating cemented detritus derived from the peloidal grainstones. The tabular shape of the rhythmites and the lack of cross-stratified structures (except local low-angle features) suggest deposition as tabular blankets. The abundant synsedimentary slumping and microfaulting in the lowermost parts of parasequences support bedding distortion and formation of some of the lowermost erosive bases (Fig. 5). The peloidal, coarsening- and thickening-upward trends of parasequences record medium-energy, subtidal conditions, shallowing upwards into higher energy, shallow-water inner-platform settings (likely foreshore), and lack evidence of subaerial exposures. The lack of skeletal material suggests that conditions were unfavourable for shelly fauna.

Carbonate sand shoals (mottled limestones)

Asymmetric parasequences (0·5–4·6 m thick), which are laterally continuous at a scale of tens of metres, coexist with slumped, contorted laminated beds, rare microfaulting, and intraclastic breccia (0·2–1·4 m thick) at their bases that are separated by erosive surfaces. These surfaces are overlain by coarsening-upward grainstone beds and lenses (*ca* 0·2–0·8 m thick), arranged into tabular to planar and trough cross-stratified, ooid-peloidal sets up to 4·6 m thick. These sets display parallel, low-angle and rippled lamination at the top. Both the contorted and bedded grainstones consist predominantly of medium-sorted peloids and ooids, with lesser amounts of coated grains, lumps, aggregates, oncoids and bioclasts (Fig. 6D). The peloids, lumps and aggregates are subangular to subrounded in shape, and up to 4 mm in diameter at the top of the parasequences. In well-preserved samples, some peloidal-like textures consist of *Proaulopora* debris, which occurs as complete or broken filaments dispersed in peloidal grainstones. Filaments are solitary, straight to slightly curved tubes, sometimes bifurcated in longitudinal section. Micritic tubes are well sorted and fragmented, and are 40–80 μm in diameter and up to 500 μm in length (Fig. 6E). The ooids (up to 1 mm in diameter) display radial, concentric or composite cortices; nuclei typically consist of micrite, micritic aggregates and intraclasts. The oncoids (up to 4 mm in size) become abundant towards the top of the parasequences; they have concentric, millimetre-thick laminae, often arranged asymmetrically, around nuclei of intraclasts and skeletal material. The fossil record occurs as nuclei of some oncoids or as uncoated, disarticulated and broken archaeocyaths and trilobite sclerites. In addition, very finely dispersed quartz and K-feldspar silt occur, increasing in abundance upwards. Some grainstone layers have isopachous cement around allochems (formed by fibrous crystals *ca* 40–50 × 400–500 μm) followed by equant spar (< 200 μm in size).

At the Tiout section, the topmost parts of some parasequences exhibit conical microbial patches (< 40 cm in diameter and up to 60 cm high) that are easily recognizable because the contorted beds lateral to these (which belong to the overlying parasequence) are commonly absent due to selective weathering (Fig. 6F). Microbial patches contain *Renalcis*, *Epiphyton* and other undeterminable thromboid textures (Fig. 7A), and numerous allochems such as oncoids and ooids locally arranged into low-angle laminae. Archaeocyathans have not been observed.

The grainstones record high-energy water conditions probably above fair-weather wave base. The parasequences are interpreted as having formed as prograding shoals on an open-marine platform suggesting deposition by storms and waves from upper shoreface to foreshore that reworked ooids, pellets, oncolites, intraclasts and fossils. The sand shoals are arranged in asymmetric, coarsening- and thickening-upward parasequences, with scoured and erosive bases, and reworking of unconsolidated to partly consolidated sediment indicating the unstable character of the substrate. At the Amouslek section, the lowermost part of parasequences lack distortion structures, and display mudstones, < 10 cm thick that record calm-water conditions in offshore settings. The fossil record is unique in that it provides evidence for the colonization of archaeocyathan and trilobite fauna. The setting of conical microbial patches at the uppermost part of parasequences indicates episodes in which the shoal bedforms ceased to migrate and were locally stabilized by microbial thromboids. Hence, episodes of decreasing energy in migrating shoals being subsequently flooded are indicated by the presence of epibenthic thromboid patches. *Proaulopora* debris did not form grain-supported fabrics within the shoals but constituted microbial bioaccumulations in high-energy environments. The possible binding role of *Proaulopora* was constrained by high-energy conditions, and the lack of self-supported structures and microbial biofilms capable of stabilizing the sediment as pointed out in other Lower Cambrian deposits (Álvaro *et al.*, 2000).

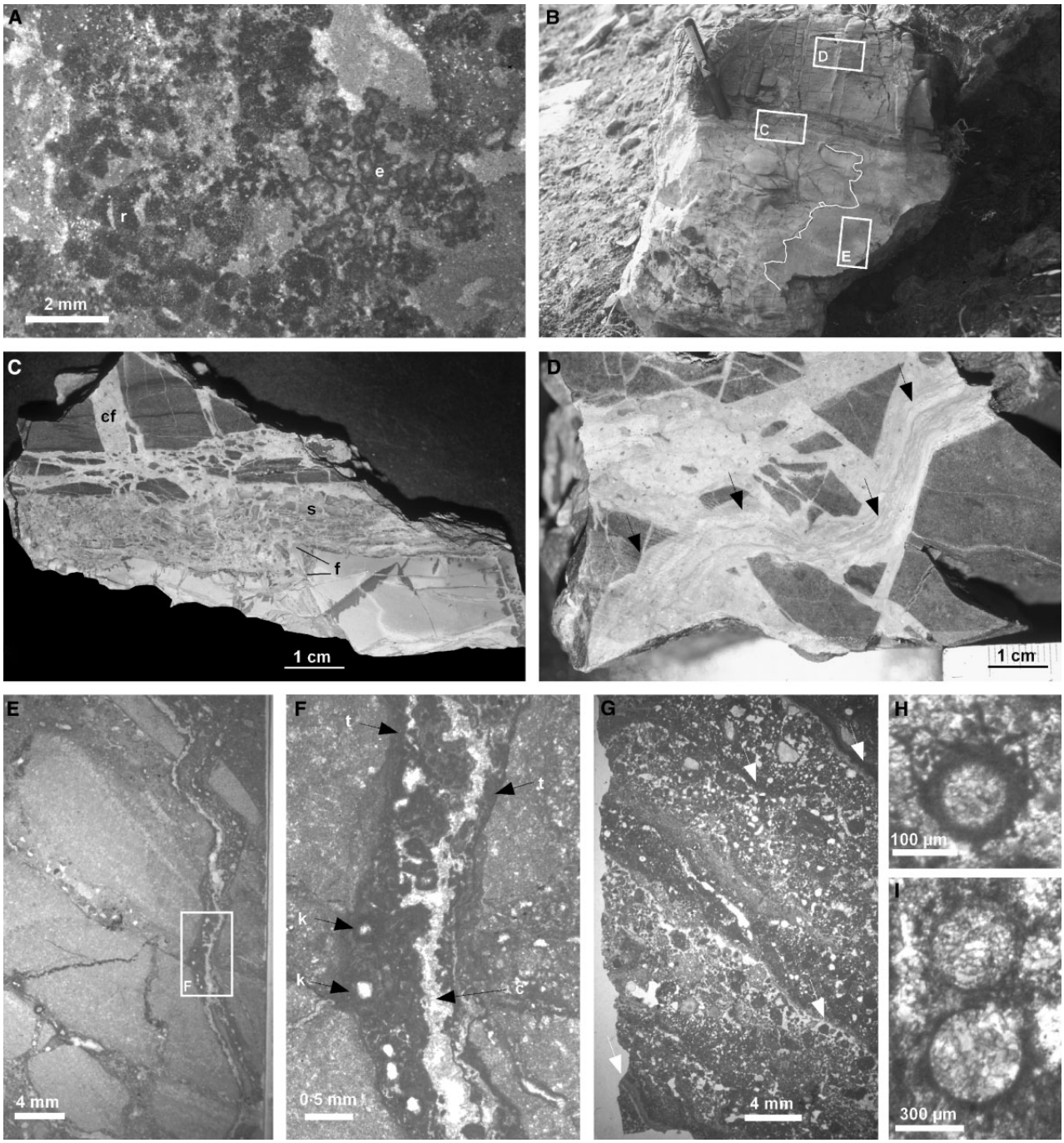

Fig. 7. (A) Microbial boundstone rich in *Epiphyton* (e) and *Renalcis* (r) of the patch shown in Fig. 6F displaying a radial arrangement of thromboids. (B–I) Cryptic cavities of Tazemmourt; (B) erosive contact of breccia (right) with the bedded peloidal rhythmites; (C) detail of fractured contact with contorted and fractured stromatolites (s), fractures (f) and cemented fissures (cf); (D) stromatolitic infill of one fissure; (E) aspect of the brecciated infill with some fissures; (F) detail of previous fissure with centripetal infill composed of undetermined thromboids (t), *Kundatia* thalli (k), and central mosaic of calcite cements (c); (G) laminated oncoidal packstones and grainstones, bounded by laminated biofilms (arrowed); (H, I) transverse sections of *Kundatia* thalli.

Cryptic fissures

The lowermost part of parasequences described in the peloidal rhythmites is locally crosscut by several generations of high-angle fissures, microfaults and cavities, forming an irregular network that stands out in contrast as irregular masses of white and reddish limestone encased in brownish

to black limestones. Individual fissures and cavities are irregular in shape and up to 1 m wide, whereas the microfault walls are straight and up to 1 cm wide (Fig. 7B–D). Most fissures and microfaults are steeply inclined, may bifurcate or anastomose, and commonly deviate significantly towards the stratification plane. They contain chaotic breccia reworked from the fissure and microfault walls, in some cases cemented and rebrecciated (Fig. 7C). The opening and brecciation of fissures were sometimes followed by growth of cavity-dwelling microbialites on the sides of the fractures, and microspar precipitation. At least two distinct filling patterns are recognized in the more complex cavities, and vary according to cavity width. The first pattern represents complete infill of open fissures and cavities > 10 cm wide, whereas the second filling pattern occurs in the thinnest microfaults. The episodic character of fracturing is evidenced by overlapping and truncation patterns displayed by the following four facies:

1 Stromatolitic crusts, up to 1 cm thick, are planar to crinkled in shape, in some cases, abruptly changing laterally into clotted-like textures. They directly encrust fissures walls (Fig. 7D).

2 Thromboid masses directly overlie the earliest generation of stromatolites. Included here are distinct thromboid structures (such as *Epiphyton*, *Girvanella*, and *Renalcis*), and other unclassified, poorly preserved, microbial remains. *Epiphyton* and *Renalcis* are common in the first millimetres as pendent fringes and masses on roofs and walls, and are arranged as rounded to irregular patches, locally displaying a somewhat laminated structure. They pass gradually centripetally into a complex framework of undetermined thromboids. Open space within this framework is filled by micropeloids (150 μm in size), quartz-rich coated aggregates (up to 3 mm in size), and micrite. Some transverse and longitudinal sections of *Kundatia* tubes (Korde, 1971) occur dispersed in the thromboid texture. These were interpreted by Buggisch & Flügel (1988) as encrusting red algae with chain-like cells arranged along the axis of the thalli. Its distinct transverse sections are circular, up to 300 μm in diameter, filled with sparry calcite and surrounded by concentric micritic haloes including very small spar-filled cells. Oblique and transverse sections exhibit peripheral spine-like processes with < 20 μm inner diameters (Fig. 7E, F, H, I).

3 Laminated peloidal/oncoidal packstones and grainstones fill the remaining voids of the larger decimetre-wide fissures and cavities. They have alternating fine- and coarse-grained laminae occurring as light to dark grey, millimetre-thick alternations (in which the angle of laminae becomes greater with proximity to the cavity walls), and common erosive contacts (Fig. 7G). The light laminae are peloidal-dominated grainstones and packstones, and contain reworked oncoids, coated intraclasts, lumps, terrigenous agglomerates, and uncoated dolomite wall-rock clasts, interbedded with isolated *Girvanella* and stratiform sheets. Relic wall particles are easily distinguished by their rusty appearance, ranging from cobble to fine-grained sand. The most obvious terrigenous fraction is angular, very fine sand to silt-size grains of quartz and feldspar, occurring both as dispersed grains (comprising 10–30% of the matrix) and as subrounded agglomerates. In contrast, the dark laminae (< 1 mm thick) are essentially stromatolitic crusts with subordinate peloids and quartz silts cemented by microsparite. Dark laminae bind the oncolitic packstone and grainstone sets and directly overlie irregular surfaces. Rounding and moderate sorting of oncoids and coated allochems filling the thicker fissures indicate influence by traction currents that reflect the hydrodynamic regime and carbonate productivity of the overlying seafloor. Evidence for episodic microbial activity occurs as variably distributed thromboid textures composed of peloids of clotted micrite, stromatolite crusts, and coated allochems. The input of allochems was episodically interrupted as indicated by nucleation of stromatolitic crusts on erosive cicatrices.

4 Sparry cement linings are sometimes present filling the remaining porosity, in some cases as a result of rebrecciation. Sparry cements usually occupy < 10% in volume. Crystals are fibrous and bladed, up to 100 × 250 μm in size.

Evidence of polyphase brecciation indicates that the fracturing process may have extended over a considerable time span. Fissures and fractures crosscut fully rigid sediments that display *in situ* brecciation. There is no evidence of karstic structures.

FACIES ASSOCIATIONS OF THE LOWER PART OF THE AMOUSLEK FORMATION

Calcareous quartz siltstones

Siltstones occur at the uppermost part (5–60 cm thick) of shale-dominated parasequences (up to

20 m thick). Tops are composed of interbedded siltstones/very fine-grained sandstones and claystones, which are rich in quartz and feldspar, and secondary pellets and peloidal aggregates. Sandstones occur as 5–30 cm thick beds and lenses, some of which are channelized. Bedforms include trough, parallel- and low-angle lamination, and wave-rippled laminae (mainly on bed tops). The laminae are commonly eroded by abundant inclined-to-subhorizontal truncation intra-surfaces dipping at 5–15°. The truncation angle is greater near the top of the beds. The contact with the underlying and interbedded shales is abrupt and erosive, and contains numerous ichnofossils such as the biostratigraphically significant ichnospecies *Psammichnites gigas* (Fig. 8A; see Álvaro & Vizcaïno, 1999, for biostratigraphic precisions). Palaeocurrents taken from foresets are 110–130°N, whereas axis channels are 25–30°N. Shales are structureless except for the presence of local centimetre-thick convolute beds.

The presence of wave-induced structures, small-scale sets of cross and parallel lamination, and channel features suggest episodes of migrating bedforms in a shoreface environment. Low-angle truncation surfaces represent reactivation surfaces resulting from reworking of bedforms by currents. The lack of mud-draped laminae and herringbone structures indicates the absence of tidal influences. On the contrary, the palaeocurrent pattern suggests the migration of superimposed bedforms in an open-sea shoreface-dominated environment. The sedimentary features of the lower shale-dominated part of these parasequences are subsequently described in detail in the open-shelf facies association.

Archaeocyathan-microbial reefs and peri-reef sediments

The term 'reef' is used in the following description because the facies association is dominated by peloidal and clotted fabrics rather than homogeneous mud fabrics. The fabrics correspond to 'Frame Reefs' (*sensu* Riding, 2002), in which in-place skeletons (including calcified microbes) are in contact and microbial clotted–peloidal fabrics are considered as microframe structures. Four geometries are distinguished: (i) patches (James & Kobluk, 1978) or isolated pillow-shaped masses ranging in size from 0·2 to 2 m and 0·2 to 1 m high, surrounded by well-bedded to massive shales; (ii) bioherms or dome- to lens-like masses of greater dimensions (but < 3·0 m thick), in which flank beds are well developed, and their margins commonly intercalate with lithologically variable inter-reef sediments; (iii) biostrome or low-relief structures (up to 1·2 m thick) comprising tabular or sheet-like beds, more than 10 m wide; and (iv) patch-reef complexes, kalyptrae complexes (*sensu* Rowland & Gangloff, 1988; Rowland & Shapiro, 2002), in which patches and bioherms occur stacked together (> 10 m thick) bounded by clay–marl–silt, millimetre- to centimetre-thick seams and discontinuities (Fig. 8B–E). The term biostrome is used here although in Cumings's (1932) original definition, a biostrome consists mainly or exclusively of the remains of organisms, and in the Kershaw's (1994) concept of 'parabiostrome' the constructing organisms are < 20% in place.

Reef-core facies

Reefs stand out in contrast as lenticular masses of white, resistant limestones encased in thinly bedded limestones and massive green shales. Reef spacing is best observed along the Tiout section, where modern differential erosion has stipped away the soft inter-reef sediments resulting in exposure of individual patches (Fig. 8D). Patches occur: (i) as single units (or individual reefs) surrounded by skeletal lime sand or homogeneous shale, (ii) arranged into stacked patches becoming aggregated into bioherms and biostromes upwards, and (iii) a complicated array of patch reefs or a kalyptrate complex caused by nucleation of numerous patches in close proximity. Where reefs are directly overlain by lime sands, the contact is commonly erosive with sands mantling a surface of truncated and disoriented archaeocyaths and surrounding lime mud.

Texturally, the reef-core facies consists of archaeocyathan–microbial boundstones and floatstones with local development of lenticular homogeneous micrite. Archaeocyaths are conspicuous contributors (see systematics in Debrenne, 1964; Debrenne & Debrenne, 1995), but they vary in abundance and some patch reefs apparently lack them. The calcified microbial community comprises *Epihyton*, *Girvanella*, *Renalcis*, and other unclassified thromboid textures (Fig. 8F–H). Their relative abundance varies from reef to reef. Other fossil remains include trilobites, chancelloriids, hyoliths, hyolithelids, sponge spicules, tannuolinids and torellellids. Peloids are major contributors to core reef facies, particularly observed when accompanied by structureless micrite. Peloidal textures consist of poorly defined, irregular silt- to sand-sized peloids of microcrystalline calcite set in a

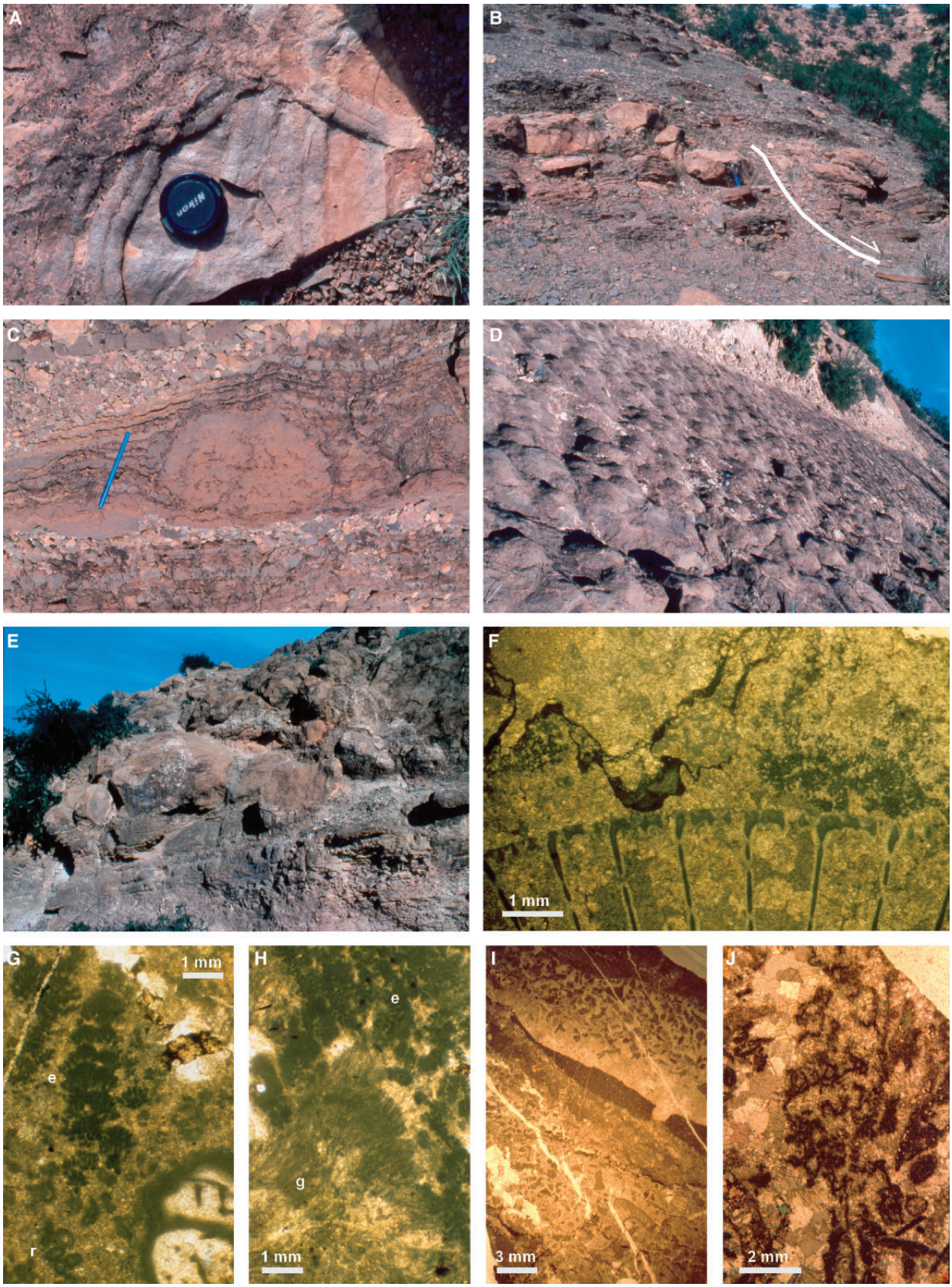
A
B
C
D
E
F
1 mm
G
1 mm
e
r
H
e
g
1 mm
I
3 mm
J
2 mm

groundmass of calcite microspar. Peloidal matrix textures grade into clotted micrite where peloid packing increases. Homogeneous micrite occurs in lenses (0·5–4 mm in diameter) or thin wavy, discontinuous laminae often inclined at various angles to the inferred depositional bedding. The laminae are less fossiliferous than the enveloping peloidal and clotted micrite fabrics. The most obvious extraclasts are angular silts of quartz and feldspars (the latter, in some cases, secondarily replaced by calcite), which make up 10–15% of the matrix. Clay minerals are present as flakes or as finely dispersed material between microspar crystals.

Flank facies

Flank beds form the margin of bioherms and, less so, the steep margins of patch reefs. They are generally thinly bedded (0·1–0·2 m) limestones that show depositional slopes. Two types of flank beds are recognized over a distance of 1–10 m: (i) beds of reef facies that thin away from the core, passing laterally into debris beds or flat bedded inter-reef sediments; and (ii) debris beds forming apron deposits around the margin of individual bioherms and patches. Debris textures contain centimetre-sized clasts of reef-core facies common in proximal positions. The skeletons and intraclasts are chaotically arranged and commonly set in a matrix of poorly sorted packstone and grainstone (with blocky cements up to 10 μm in size), the latter bearing dispersed *Girvanella* bundles and biodictyon (*sensu* Krumbein *et al.*, 2003; Fig. 8I, J). Low-angle scour surfaces within flank sediments attest to the episodic erosion of the reef surface that was responsible for generating the intraclasts present in debris beds and proximal inter-reef sediments.

The dip of the flanks varies from 5° to 40°, so that flanking-slope grainstones and packstones attest to development of significant syndepositional relief on some bioherms. As steep (up to 40°) depositional slopes were developed, much debris was shed during intermittent erosive episodes and deposition on flanks. Geopetal structures indicate that some skeletons were secondarily reworked.

Inter- and off-reef sediments

Inter-reef sediments are dominated by bedded calcarenites that can extend out from the reefs and grade over < 3 m into nodular limestones, shales bearing centimetre-thick limestone nodules paralleling stratification, and ultimately claystones. In the absence of calcarenites, the patches and bioherms are directly surrounded by off-reef green shales with isolated centimetre-thick carbonate nodules. Inter-reef calcarenites and nodular limestones show local packstone and bioturbated wackestone textures. They contain a diverse fauna comprising reworked archaeocyaths, trilobites, brachiopods, hyoliths and chancelloriid sclerites. The nature of inter-reef sediments in each reef complex provides insight into the prevailing water conditions. The dominant wackestones, nodules and thin beds interbedded with shales suggest deposition in quieter and/or deeper water environments with a minor siliciclastic supply. Inter- and off-reef sediments are indicative of low-energy water environments, although minor scours at the base of the wackestones together with reef-related intraclasts (up to 2 cm in size) suggest episodic reworking.

Size, spacing and distribution of reefs appear to have controlled the nature of inter-reef sediments, which vary from wakestones, packstones to claystones. The variability in inter-reef sediment records a wide range of hydrodynamic conditions during deposition. Individual reefs influenced the local hydrodynamic regime, and were sufficiently coherent to withstand fairly turbulent conditions. However, they were subject to episodic erosion as indicated by the abundance of lithified intraclasts in adjacent flank and inter-reef facies and erosive surfaces within the reefs. The sharp contact between reefs and their surrounding sediments, the high-angle nature of many of the flanks and their microfacies indicate an important early diagenetic consolidation. This rigidity is important because it permitted development of steep slopes and preserved the lenticular shape of patches and bioherms. In addition, the lack of bioturbation in the reef-core and flank facies suggests that microbially controlled substrate consistency was a major control on the

Fig. 8. (A) *Psammichnites gigas* preserved as convex epireliefs in calcareous quartz siltstones at Tazemmourt; (B) slumped patches (right) at Tazemmourt; (C) isolated archaeocyathan–microbial patch surrounded by laminated alternations of limestones and shales at Tiout; (D) bedding surface at Tiout showing the lateral distribution of archaeocyathan–microbial patches; (E) kalyptrate complex at Tiout with vertical arrangement of patches and bioherms; (F) *Epiphyton* thromboid (right) encrusting an archaeocyathan wall; (G) *Epiphyton* (e) bushes and *Renalcis* clots (r); (H) *Girvanella* (g) and *Renalcis* thromboids; (I) alternations of bioclastic grainstone and eroded mudstone-wackestone, biohermal flank; (J) *Girvanella*-like filaments in a grainstone flank.

composition of the reef biota. Trapping and binding of sediment on the surface of the reef cores resulted in steep depositional slopes and flanks. The cores supported steep-sided erosive scours on their tops indicating that they could withstand deposition in a predominantly high-energy environment. The abundance of microbial activity (recorded as thromboid textures, biodictyon, and micritized grains and bioclasts), shelter cements and lack of bioturbation indicate abundant early lithification.

The reef and peri-reef sediments are characteristically rhythmic displaying individual parasequences that, in some cases, can only be correlated laterally to up to 50 m. Each shallowing-upward parasequence (5–20 m thick) comprises a basal shale unit that contains carbonate nodules that increase in number upwards. This facies is overlain by nodular limestones, and uppermost patch reefs passing upwards into bioherms, biostromes and kalyptrae. Influx of quartz and feldspar silt reflects exposure of the interior platform source region. Slump structures that incorporate individual patches indicate the existence of steep-sided reef morphologies and unstable, soft clay substrates (Fig. 8B). The lack of lateral continuity of the parasequences indicates that conditions for reef nucleation were not widely developed probably due to differences in accommodation space.

Open-shelf sediments

Green shales form the bulk of the unit and are dominated by fine quartz and angular feldspar silt (the latter locally up to 60% in volume), sericite, illite, and muscovite flakes. Fossil fauna is sporadically abundant, preserved as articulated, disarticulated and broken debris, and comprises trilobites, echinoderm ossicles, brachiopods and hyoliths. Despite the massive aspect of the shales, their stratification is suggested by millimetre-thick, finely crinkled, silty laminae and the layering of centimetre-thick carbonate nodules. Centimetre-thick, grey siltstone intercalations exhibit erosive bases and grading. Centimetre-thick, limestone nodules contain bioclastic packstones–wackestones (changing upwards from skeleton- to claystone-supported) that rest upon sharp erosive bases, which display common gutter marks. The fossil content is similar to that described in shales, but is predominantly fragmented and highly abraded. Finally, scattered soft-sediment deformation structures also occur in many beds in the form of intraformational slumping and sliding structures, up to 0·6 m thick, and lithologically similar to the underlying beds.

This facies association was deposited on offshore substrates, under calm-water conditions as evidenced by the dominance of siliciclastic mud and episodic preservation of a partially articulated shelly fauna. The interbedded siltstones and limestones were probably introduced as a result of storm surges, as indicated by the presence of erosive bases, grading and fragmented skeletons. Thus, this is interpreted as an environment characterized by continuous deposition below fair-weather conditions that was punctuated by storm-induced episodes. Slumping and synsedimentary bedding distortion of the substrate resulted in local sliding and plastic sediment masses.

DEPOSITIONAL TRENDS

According to a proximal-to-distal facies distribution and the Cambrian palaeogeographic reconstructions proposed by Destombes *et al.* (1985) and Geyer *et al.* (1995) for the Souss Basin, relatively proximal facies occur at the Tiout section, whereas distal sediments are distributed along a transect between the Tazemmourt and the Amouslek sections. The pattern of deposition across the Tiout/Amouslek lithostratigraphic transition is punctuated by two major stratigraphic discontinuities (D_1 to D_2 in Fig. 4).

Discontinuity D_1 is located at the top of the above-reported peloidal rhythmites and stromatolitic reefs (Tiout Member). At the Tiout section, this sharp erosive contact marks the base of the *Eofallotaspis* trilobite zone. This contrast represents a distinct facies shift from tabular peloidal rhtyhmites changing laterally into coeval peritidal stromatolitic reefs to an intra-shelf ramp with ooid/bioclastic shoals. Discontinuity D_2 is placed at the Tiout/Amouslek lithostratigraphic contact (according to the amended lithostratigraphy), and appears as a rectilinear surface of erosion with small-scale irregularities. D_2 marks the bottom of the *Eofallotaspis* zone outside the Tiout section, and is overlain by the transgressive Amouslek Formation, characterized by siliciclastic input and open-sea offshore conditions. Both discontinuities show a widespread distribution in the whole Anti-Atlas, reflected by the common inclusion of the Tiout Member in recent geological maps (Chalot-Prat *et al.*, 2001; Gasquet *et al.*, 2001).

The facies distribution of the Tiout/Amouslek lithostratigraphic transition throughout the whole western Anti-Atlas can be related to three discontinuity-bounded facies associations that are arranged in a broad retrogradational (transgressive) trend. This succession can be subdivided into vertically stacked, asymmetrical parasequences exhibiting either conformable or erosive contacts. The peloidal–stromatolite sedimentary system is composed of successive shallowing-upward parasequences (0·1–1·2 m thick), which include the aforementioned stromatolitic reefs and peloidal rythmites. The bases of the parasequences are flooding surfaces, whereas their tops are bounded by minor discontinuities (tp in Fig. 4). Discontinuities are directly overlain by reworked intraclasts, microfaulting and minor slumps. Discontinuity D_1 marks a sharp sedimentologic change, as it marks the end of a stromatolite-dominated system and the establishment of open-sea conditions related to the immigration of shelly fossils. Parasequences (0·5–4·6 m thick) in the stratigraphic level are dominated by ooid-dominated grainstones (shoreface shoals) that contain the first biostratigraphically significant shelly fossils (Sdzuy, 1978). D_2 marks the beginning of a broad transgression of the platform, recorded by shallowing-upward parasequences (up to 20 m thick) of the Amouslek Formation. These, in turn, are topped by either calcareous quart siltstones or archaeocyathan–microbial reef systems. The rhythmic sedimentation of the Amouslek Formation represents a gradual deepening of the platform culminating with flooding and blanketing of the whole platform by fine-grained terrigenous material.

One important implication of this analysis is the character of the base of the *Eofallotaspis* zone. This interval is properly identifiable at the Tiout section overlying discontinuity D_1, but it is diachronously correlatable in other outcrops overlying discontinuity D_2 as a result of sampling biases.

FACTORS CONTROLLING REPLACEMENT OF REEF-BUILDING CONSORTIA

The aforementioned facies spatial patterns are related to the successive establishment of three main reef-building benthic communities (Fig. 9). The oldest reef-building community is the frame-building stromatolite-dominated system. The youngest stromatolite-thrombolite consortium that dominated the western Souss platform across the Neoproterozoic–Cambrian transition (Adoudou, Lie-de-vin and lower member of the Igoudine formations) is recorded in the studied area by stromatolite reefs flourishing on a peritidal platform that record repeated substrate instability. A distinct microbial community episodically developed within cryptic fissures, cracks and microfaults located at the lowermost part of the parasequences reported in the Tiout Member. Fissures provided habitats for pioneer coelobiontic organisms that directly encrusted cavity walls and roofs, even after their reactivation by synsedimentary fracturing. The coelobiontic community was relatively diverse and consisted of encrusting, self-supported chemosynthetic–heterotrophic microbial communities, including stromatolitic crusts, *Renalcis–Epiphyton* intergrowths, and *Kundatia* algae(?) (the algal affinity of the latter is open to discussion due to its presence in cryptic fissures). The multiple generations of high-angle fractures indicate a brittle deformation at the onset of cavity fillings, suggesting that the polyphase filling of cavities was controlled by displacements on nearby microfaults. The aforementioned penecontemporaneous fissures, breccias, crackage and microfaults can be developed in response to overall differential subsidence. Their setting seems to be facies- and parasequence-controlled, and does not require any regional tectonism. One distinct factor that controlled the infill of larger cavities was local hydrodynamic conditions determined in part by surrounding submarine topography. The main phase of hydrodynamic filling is associated with reworked 'oncolitized' extra- and intraclasts washed in from an overlying, unpreserved substrate. Crucial prerequisites for microbial colonization within the thinnest (< 1 cm wide) and deepest fissures include the presence of water, and the potential of the habitats to support microbial growth and proliferation related to chemoautotrophic microbial mats. These mats have yielded a rich supply of organic compounds to nourish possible heterotrophs. The microbial coelobiontic communities described above are relatively diversified if compared with other Lower Cambrian metazoan-rich coelobiontic communities (Kobluk, 1988; Vennin *et al.*, 2003).

The second stage of reef-building benthic communities was the frame-building pioneer thrombolite–archaeocyathan consortium. Overlying D_1, a shoal belt dominated by cross-bedded grainstones developed locally proximal to the transect of the Amouslek–Tiout–Tazemmourt sections. These

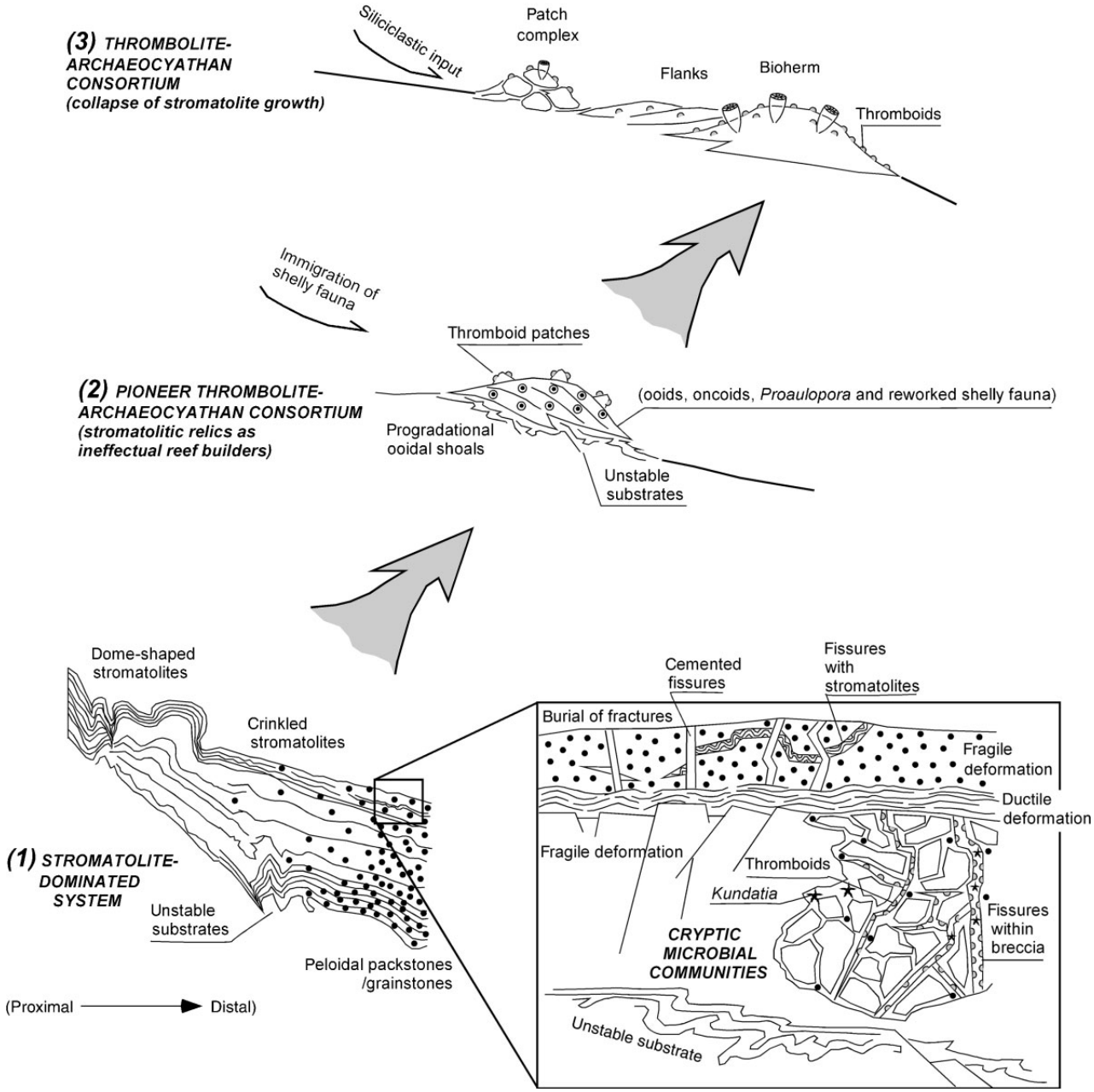

Fig. 9. Evolution of reef-building consortia during Early Atdabanian times in the western Souss platform (not to scale).

shoals were adjacent to a shelly benthic community (probably reefal in character) represented by reworked (allochthonous) archaeocyathans and trilobites. This biotic assemblage represents the oldest biostratigraphically significant Early Cambrian shelly fossils from Morocco. Thromboid-rich patches occur on the top of ooid-dominated parasequences, reflecting episodes of decreasing hydrodynamic energy over migrating shoals, and epibenthic thromboid colonization of relative stable substrates. By contrast, the shoals are evidence of development of ineffectual-builder biofilm relics (oncoids), deposition of microbial (*Proaulopora*) bioaccumulations and reworked archaeocyaths. Archaeocyaths, not preserved in life position, could colonize either the conical thromboid patches or laterally equivalent, back-shoal, trombolite–archaeocyathan reefs.

The final stage of frame-building benthic communities is the thrombolite–archaeocyathan consortium. Subsequent transgression resulted in deposition of fine-grained siliciclastic material and the immigration of open-sea shelly faunas in the whole western Souss platform. The change in

habitat seems to have supported a broad migration of shelly fauna onto the whole western Souss platform, and the final collapse of flat-laminated microbial mat growth. The fine peloidal and clotted nature of the reef micrite is apparently at variance with the prevailing moderate to high energies indicated by well-sorted, cross-bedded, inter-reef lithologies, suggesting some stabilizing biotic influence, as well as early cementation. The microbial communities probably formed a mat across the surface of both reef cores that trapped and bound the fine skeletal debris washed onto the surface, and their flanks. Rapid cementation, microbial binding and hence internal stabilization of reef fabrics would have prevented compaction and promoted steep depositional dips. The reported reef parasequences of the Amouslek Formation indicate shallowing-upward trends reaching fair-weather base, as suggested by the associated intraclasts and sedimentary structures.

The vertical architecture of the overlying Amouslek Formation is the result of variations in relative sea level leading to the establishment of nucleation sites for the succeeding benthic community composed of archaeocyathan–microbial reefs. The carbonate platform recorded development of archaeocyathan–microbial reefs that covered, with their detritus, increasingly expanding sectors of the seafloor. The associated transgressive trend accompanied dramatic biotic radiation by increasing habitat size, and allowing shelly metazoans (including frame-building organisms) to invade platform interiors.

Reef geometries were influenced by substrate stability, water depth, subsidence rate, and local hydrodynamic conditions. In areas of relatively shallow water and slow subsidence rates, reefs grew by lateral accretion and amalgamation developing low-relief biostromes (i.e. patches are always overlain by biostromes). In areas of higher subsidence, vertical growth of reefs was less constrained, and they developed predominantly by vertical accretion as bioherms. Because of a marked tendency for aggregation and consequent formation of patch complexes or kalyptrae in the Amouslek Formation, the dimensions of their individual patches and bioherms are often difficult to determine.

CONCLUSIONS

The Tiout–Amouslek lithostratigraphic transition (early Atdabanian in age) of the western Anti-Atlas records one of the most significant Lower Cambrian benthic communities related to the Cambrian explosion. When shelly metazoans arrived in the western Souss endemic platform, they proliferated to the detriment of the stromatolite-dominated frame-building community that flourished across the underlying Adoudou, Lie-de-vin formations and the lower member of the Igoudine Formation. The Early Atdabanian transgression led to habitat destruction and environmental perturbation. The invasion of shell taxa can be viewed as a primary result of this transgression leading to the establishment of a reef fringe on this part of the western Gondwana margin. Three stages of reef-building microbial-dominated benthic communities are distinguished, from stromatolite-dominated to thrombolite–archaeocyathan consortia. The latter records the abrupt collapse of stromatolite growth.

An archaeocyathan–thrombolite consortium displaced the stromatolite-frame-building assemblages in the Siberian platform-reef settings at the base of the Tommotian. Although this metazoan–calcimicrobe reef-building consortium did not range beyond the Siberian platform during the Tommotian (Zhuravlev, 1986), during the Atdabanian and Botoman the archaeocyathan–thromboid reef-building consortium spread from the Siberian platform to sites along the Gondwana margin. Across the Atdabanian-Botomian transition the archaeocyathan–thromboid reef-building consortium had spread to North America and Australia (Rowland & Shapiro, 2002). In the western Souss platform, the immigration of Ediacaran and pre-Atdabanian early shelly fossils is not recorded due to ecological restricted conditions that disappeared associated with the establishment of the Atdabanian stratigraphic discontinuity D_1.

In summary, the stratigraphically abrupt appearance of the earliest Cambrian shelly fauna within the Tiout shoals reflects changes in the sedimentary patterns of the western Souss platform. The previous western Souss platform probably had poor circulation and restricted exchange with surrounding basinal areas, whereas the Tiout shoals record a depositional setting open to oceanic water circulation, probably adjacent to an oceanic basin. Differential subsidence of the carbonate platform and transgression may have enabled improved water circulation over carbonate platform interiors in the Atdabanian. Conditions over the carbonate platform may therefore have been more open marine during the Early Atdabanian allowing the succeeding microbial and archaeocyathan–microbial

reefs to colonize shelf-interior settings. Episodic instability of the seafloor, which may be tectonically induced, favoured the growth of coelobiontic communities below the Tiout/Amouslek lithostratigraphic contact and archaeocyathan–microbial reefs in the overlying Amouslek Formation.

ACKNOWLEDGEMENTS

The authors warmly acknowledge the constructive criticism made by I. Montañez, R. Riding and an anonymous referee, who have greatly improved the ideas expressed in the manuscript, and the advice and comments made by J. Destombes, J. M. Rouchy and E. Vennin. The outcrops were visited by the ISCS in 1995. Research has been supported by ECLIPSE project 'Evolution of Biogeochemical Cycles from Archean to Recent Environments', and is a contribution to IGCP project 485 'Cratons, Metacratons and Mobile Belts: Keys from the West African Craton Boundaries, Eburnian versus Pan-African Signature, Magmatic, Tectonic and Metallogenic Implications'.

REFERENCES

Álvaro, J.J. and **Vizcaïno, D.** (1999) Biostratigraphic significance and environmental setting of the trace fossil *Psammichnites* in the Lower Cambrian of the Montagne Noire (France). *Bull. Soc. géol. France*, **170,** 821–828.

Álvaro, J.J., Vennin, E., Moreno-Eiris, E., Perejón, A. and **Bechstädt, T.** (2000) Sedimentary patterns across the Lower-Middle Cambrian transition in the Esla nappe (Cantabrian Mountains, northern Spain). *Sed. Geol.*, **137,** 43–61.

Álvaro, J.J., Elicki, O., Geyer, G., Rushton, A.W.A. and **Shergold, J.H.** (2003) Palaeogeographical controls on the Cambrian trilobite immigration and evolutionary patterns reported in the western Gondwana margin. *Palaeogeogr. Palaeoclimat. Palaeoecol.*, **195,** 5–35.

Boudda, A., Choubert, G. and **Faure-Muret, A.** (1979) Essai de stratigraphie de la couverture sédimentaire de l'Anti-Atlas: Adoudounien – Cambrien inférieur. *Notes Mém. Serv. Géol. Maroc*, **271,** 1–96.

Buggisch, W. and **Flügel, E.** (1988) The Precambrian/Cambrian boundary in the Anti-Atlas (Morocco). Discussion and new results. *Lect. Notes Earth Sci.*, **15,** 81–90.

Chalot-Prat, F., Gasquet, D., Roger, J., Hassenforder, P., Chevremont, P., Baudin, T., Razin, P., Benlakhdim, A., Benssaou, M. and **Mortaji, A.** (2001) *Carte géologique du Maroc au 1/50 000. Feuille de Sidi Bou'Addi. Mémoire explicatif*. 84 pp. Eds. Serv. Géol. Maroc.

Choubert, G. (1952) Histoire géologique du domaine de l'Anti-Atlas. In: *Géologie du Maroc. XIX Congrès Géol. Intern., Alger 1952* (Eds G. Choubert and J. Marçais), *Monogr. Rég., Sér. 3, Maroc*, **6,** 77–194. 16 maps. Alger.

Choubert, G. (1953) Le Précambrien III et le Géorgien de l'Anti-Atlas. *Notes Mém. Serv. Géol. Maroc*, **103,** 7–39.

Clauer, N., Caby, R., Jeanette, D. and **Trompette, R.** (1982) Geochronology of sedimentary and metasedimentary rocks of the West African Craton. *Precambrian Res.*, **18,** 53–71.

Cumings, E.R. (1932) Reefs or bioherms? *Bull. Geol. Soc. Am.*, **43,** 331–352.

Debrenne, F. (1964) Archaeocyatha. Contribution à l'étude des faunes cambriennes du Maroc, de Sardaigne et de France. *Notes Mém. Serv. Géol. Maroc*, **179,** 1–265.

Debrenne, F. and **Debrenne, M.** (1995) Archaeocyaths of the Lower Cambrian of Morocco. *Beringeria (Special Issue)*, **2,** 121–145.

Destombes, J., Hollard, H. and **Willefert, S.** (1985) Lower Palaeozoic rocks of Morocco. In: *Lower Palaeozoic Rocks of the World. Vol. 4. Lower Palaeozoic of North-western and West Central Africa* (Ed. C.H. Hollard), pp. 157–184. John Wiley and Sons, Chichester.

Gasquet, D., Roger, J., Chalot-Prat, B., Hassenforder, B., Baudin, T., Chevremont, P., Razin, P., Benlakhdim, A., Mortaji, A. and **Benssaou, M.** (2001) *Carte géologique du Maroc au 1/50 000. Feuille de Tamazrar. Mémoire explicatif*. 95 pp. Eds. Serv. Géol. Maroc.

Geyer, G. (1989) Late Precambrian to Early Middle Cambrian lithostratigraphy of southern Morocco. *Beringeria*, **1,** 115–143.

Geyer, G. (1990) Revised Lower to lower Middle Cambrian biostratigraphy of Morocco. *Newsl. Stratigr.*, **22,** 53–70.

Geyer, G., Landing, E. and **Heldmaier, W.** (1995) Faunas and depositional environments of the Cambrian of the Moroccan Atlas region. *Beringeria (Special Issue)*, **2,** 47–120.

Houzay, J.P. (1979) Empreintes attribuables à des méduses dans la série de base de l'Adoudounien (Précambrien terminal de l'Anti-Atlas, Maroc). *Géol. Méditerr.*, **6,** 379–384.

Hupé, P. (1953) Contribution à l'étude du Cambrien inférieur et du Précambrien III de l'Anti-Atlas marocain. *Notes Mém. Serv. Géol. Maroc*, **103** (1952), 1–362.

James, N.P. and **Kobluk, R.** (1978) Lower Cambrian patch reefs and associated sediments: southern Labrador, Canada. *Sedimentology*, **25,** 1–35.

Kershaw, S. (1994) Classification and geological significance of biostromes. *Facies*, **31,** 81–92.

Kirshvink, J.L., Magaritz, M., Ripperdan, R.L. and **Zhuravlev, A.Yu.** (1991) The Precambrian/Cambrian boundary: Magnetostratigraphy and carbon isotopes resolve correlation problems between Siberia, Morocco, and South China. *GSA Today*, **1,** 69–71.

Kobluk, D.R. (1988) Cryptic fauna in reefs: ecology and geologic importance. *Palaios*, **3,** 379–390.

Korde, K.B. (1971) Vodorosli kembriya. *Akad. Nauk SSSR, Trudy Paleont. Inst.*, **139,** 1–349 (in Russian).

Krumbein, W.E., Brehm, U., Gerdes, G., Gorbushina, A.A., Levit, G. and **Palinska, K.A.** (2003) Biofilm, biodictyon, biomat microbialites, oolites, stromatolites geophysiology, global mechanism, parahistology. In: *Fossil and Recent Biofilms. A Natural History of Life on Earth* (Eds W.E. Krumbein, D.M. Paterson and G.A. Zavarin), pp. 1–28. Kluwer, Dordrecht.

Latham, A. and **Riding, R.** (1990) Fossil evidence of the location of the Precambrian/Cambrian boundary in Morocco. *Nature*, **344,** 752–754.

Leblanc, M. and **Lancelot, J.R.** (1980) Interprétation géodynamique du domain panafricain (Précambrien terminal) de l'Anti-Atlas (Maroc) à partir de données géologiques et géochronologiques. *Can. J. Earth Sci.*, **17,** 142–155.

Magaritz, M., Kirshvink, J.L., Latham, A.J., Zhuravlev, A.Yu. and **Rozanov, A.Yu.** (1991) Precambrian/Cambrian boundary problem: Carbon isotope correlations for Vendian and Tommotian time between Siberia and Morocco. *Geology*, **19,** 847–850.

Monninger, W. (1979) The section of Tiout (Precambrian/Cambrian boundary beds, Anti-Atlas, Morocco): an environmental model. *Arb. Paläont. Inst. Würzburg*, **1,** 1–289.

Narbonne, G.M., Landing, E. and **Anderson, M.M.** (1987) A candidate stratotype for the Precambrian-Cambrian boundary, Fortune Head, Burin Peninsula, southeastern Newfoundland. *Can. J. Earth Sci.*, **24,** 1277–1293.

Riding, R. (2002) Structure and composition of organic reefs and carbonate mud mounds: concepts and categories. *Earth-Sci. Rev.*, **58,** 163–231.

Rowland, S.M. and **Gangloff, R.A.** (1988) Structure and paleocology of Lower Cambrian reefs. *Palaios*, **3,** 111–135.

Rowland, S.M. and **Shapiro, R.S.** (2002) Reef patterns and environmental influences in the Cambrian and earliest Ordovician. *Soc. Econ. Paleont. Miner. Spec. Publ.*, **72,** 95–128.

Schmitt, M. (1979) The section of Tiout (Precambrian/Cambrian boundary beds, Anti-Atlas, Morocco): stromatolites and their biostratigraphy. *Arb. Paläont. Inst. Würzburg*, **2,** 1–188.

Sdzuy, K. (1978) The Precambrian-Cambrian boundary beds in Morocco (preliminary report). *Geol. Mag.*, **115,** 83–94.

Spizharski, T.N., Zhuravleva, I.T., Repina, L.N., Rozanov, A.Yu., Tchernysheva, N.Ye. and **Ergaliev, G.H.** (1986) The stage scale of the Cambrian System. *Geol. Mag.*, **123,** 387–392.

Tucker, E. (1986) Carbon isotope excursions in Precambrian/Cambrian boundary beds, Morocco. *Nature*, **319,** 48–50.

Van Wagoner, J.C., Posamentier, H.W., Mitchum, R.M., Vail, P.R., Sarg, J.F., Loutit, T.S. and **Hardenbol, J.** (1988) An overview of the fundamentals of sequence stratigraphy and key definitions. In: *Sea-Level Changes – An Integrated Approach* (Eds C. Wilgus, B. Hastings, C. Ross, H. Posamentier, J. Van Wagoner and L.G.St.C. Kendall). *Soc. Econ. Paleont. Miner., Spec. Publ.*, **42,** 39–45.

Vennin, E., Álvaro, J.J., Moreno-Eiris, E. and **Perejón, A.** (2003) Lower Cambrian coelobiontic communities in tectonically unstable crevices developed in Neoproterozoic volcanics, Ossa-Morena, southern Spain. *Lethaia*, **36,** 53–65.

Zhuravlev, A.Yu. (1986) Evolution of archaeocyaths and paleobiogeography of the Early Cambrian. *Geol. Mag.*, **123,** 377–385.

Zhuravlev, A.Yu. and **Riding, R.** (Eds.) (2001) *The Ecology of the Cambrian Radiation*. Columbia University Press, New York, 525 pp.

Manuscript received 16 April 2004; revision accepted 26 June 2005.